

Performance Characteristics of Cylindrical Hall Thrusters

IEPC-2009-094

*Presented at the 31st International Electric Propulsion Conference,
University of Michigan • Ann Arbor, Michigan • USA
September 20 – 24, 2009*

Seongmin Kang¹, Younho Kim², Yunhwang Jeong³
Satrec Initiative, Daejeon, 305-811, Korea

Jongho Seon⁴
Kyunghee University, Yongin, 446-701, Korea

and

Jongsub Lee⁵, Mihui Seo⁶, Wonho Choe⁷
KAIST, Daejeon, 305-701, Korea

Abstract: A low power Hall thruster is under development for orbit maintenance of a small Earth observing satellite. To characterize the performance of cylindrical Hall thrusters both cylindrical and annular type thrusters were tested and the results were described through comparative analyses. Cylindrical thrusters were manufactured in two different channel diameter dimensions, 28 mm and 50 mm to study the performance dependence on channel sizes. Thrust, ion velocity and ion current were measured in various operating conditions. The results show that cylindrical thrusters are more efficient in mass utilization and voltage utilization, but less efficient in current utilization than annular one.

Nomenclature

V_D = discharge voltage
 V_K = keeper voltage
 V_H = heater voltage

I. Introduction

THE cylindrical Hall thruster can be a candidate of low power propulsion devices for orbit maintenances of small Earth observing satellites. The cylindrical Hall thruster (CHT) has been first designed by Princeton Plasma Physics Laboratory (PPPL) to make up for weak points of conventional annular Hall thrusters in small dimension and low power.¹⁻⁴ The performance requirement specifications of our propulsion subsystem are 10 mN thrust, 1200 s specific impulse and 30% anode efficiency at an anode power of 200 W. To meet the requirement we consider two types of Hall thrusters, that is, the cylindrical type Hall thruster and the conventional annular type thruster. Three laboratory models of thrusters were manufactured and tested. They are SI-200Cv1, SI-200Cv2 and SI-200Av1. SI-

¹ Research Engineer, R&D Center, smkang@satreci.com.

² Research Engineer, R&D Center.

³ Chief Research Engineer, R&D Center.

⁴ Associate Professor, Department of Astronomy and Space Science.

⁵ Ph.D Candidate, Department of Physics.

⁶ Ph.D Candidate, Department of Physics.

⁷ Professor, Department of Physics.

200Cv1 is a cylindrical type thruster with a channel diameter of 28 mm, SI-200Cv2 is a cylindrical type thruster with a channel diameter of 50 mm, and SI-200Av1 is an annular type thruster with a channel diameter of 50 mm. In our study cylindrical thrusters needed stronger magnetic field, so consumed more magnet power than the annular thruster. In this study the power consumption by magnets was excluded from the efficiency analysis and also cathode power and cathode fuel supply were not considered. The anode efficiency was decomposed by four utilization efficiencies, that is, mass utilization, current utilization, voltage utilization and charge utilization. Each of utilizations was defined by the following way.⁵

1. The mass utilization is the conversion of neutral mass flow rate into ion mass flux.
2. The current utilization is the fraction of ion current in the discharge current.
3. The voltage utilization is the conversion of discharge voltage into ion velocity.
4. The charge utilization is the fraction of multiply-charged ions in the plasma.

II. Experiments

A. Thrusters

The mechanical schematic of the SI-200Cv2 thruster is shown in Fig. 1. The channel is fully cylindrical and is separated into two parts, that is, an outer wall and an inner wall. The material of channel wall is boron nitride. The channel diameter is 50 mm and the channel length is 24 mm. The magnetic circuit includes two electromagnetic coils which are connected to separate power supplies. One is wound outside the outer channel and the other is inside the inner channel consisting of a core of pure iron. The side coil was designed to control the magnetic field inside the channel globally and it consumes the greater part of the magnet power, while the center coil controls the local magnetic field near the center of inner channel wall where the magnetic mirror effect of electrons works. The magnetic mirror effect is one of the electron confinement mechanisms in cylindrical Hall thrusters.⁶ The calculated magnetic field lines and an axial profile of magnetic flux density are shown in Fig. 2.⁷

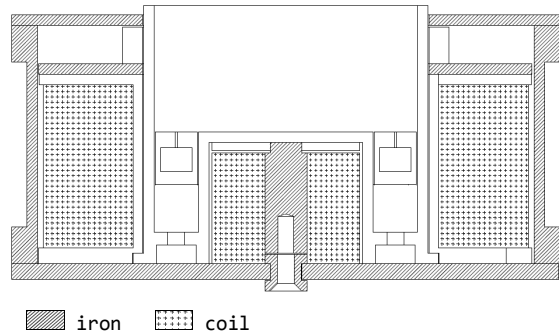


Figure 1. Mechanical design for the SI-200Cv2.

The SI-200Av1 thruster is a conventional annular type Hall thruster with the similar channel structure like the Russian stationary plasma thruster SPT-50.⁸⁻⁹ The channel was made of boron nitride same as the SI-200Cv2, with an external diameter of 50 mm and an internal diameter of 28 mm. The anode was mounted at 25 mm from the channel exit. The magnetic circuit included four side coils outside the outer channel wall and one center coil inside the inner channel wall. To control the magnetic field distribution the side coils and the center coil were fed from two separate power supplies.

A commercial hollow cathode (Heatwave, HWPES-250) is used to neutralize the ion beam. This cathode is

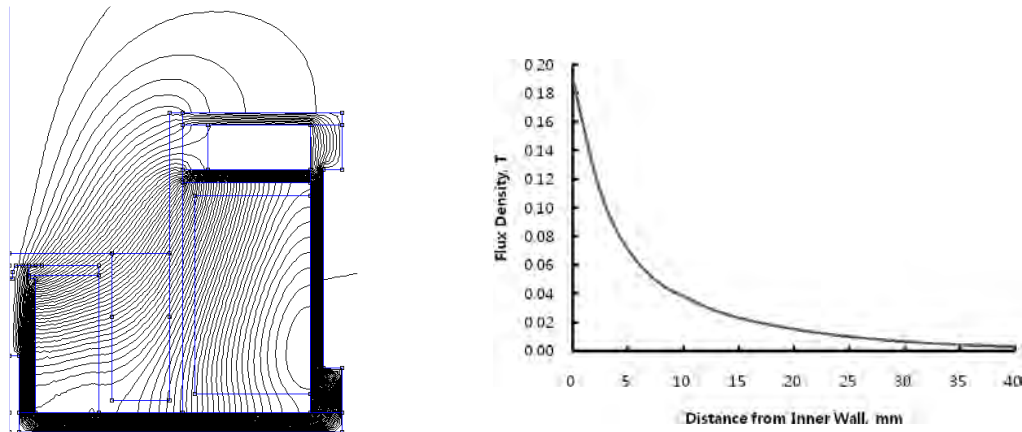


Figure 2. Sectional view of magnetic field structure and flux density curve at thruster axis.

positioned about 5 cm downstream of the channel exit plane. The operating parameters of the tests for cylindrical thrusters include a xenon flow rate of 0.5-0.7 mg/s, a side coil current of 1 A, a center coil current of 4 A, discharge voltage of 125-350 V and a cathode flow rate of 0.1 mg/s.

B. Vacuum facility and diagnostics

All the thrust measurements and diagnostics of thrusters were performed in a 1.9 m long stainless vacuum chamber with diameter of 1 m. During nominal operation of the thruster, the pressure inside the chamber is kept to approximately 7×10^{-5} torr by two cryopumps and five turbopumps. Separate DC power supplies are used for the discharge, electromagnetic coils, cathode keeper, and cathode heater. As shown in Fig. 3 the common ground of thruster circuit was connected to the chamber wall through a resistor to monitor the ground current. It is thought that the ground current become zero when the ion beam is completely neutralized. After the thruster ignition, keeper power supply can be used to control the amount of electron emission from the cathode.

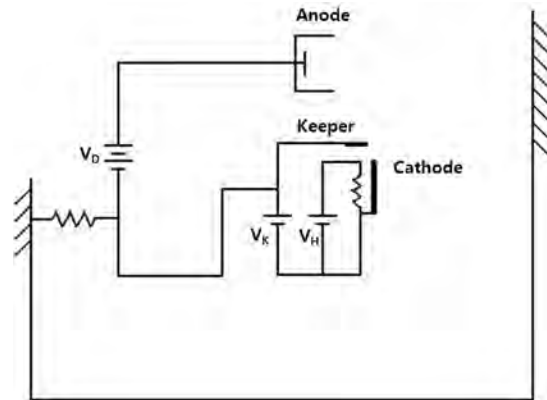


Figure 3. Electric circuit diagram. V_D denotes the discharge voltage, V_K denotes the keeper voltage, and V_H denotes the heater voltage.

Thrust was measured by a pendulum type thruster stand. The displacement of the pendulum was converted into a proportional voltage signal by a position sensitive device (PSD). In situ calibrations were performed using three weights of known masses. Multiple thrust measurements and calibrations in various operating condition have demonstrated that the system has a standard error of less than 0.1 mN.

The Faraday probe measured ion beam current of the thruster. The probe was located 38 cm downstream of the thruster exit plane, mounted on a rotary translation stage. The beam current density was measured in the range of -90 to 90 degree. The retarding potential analyzer (RPA) was used to generate the ion energy distribution. We analyzed the efficiency, breaking it down to mass utilization, current utilization and voltage utilization using the measured data. However, the analysis was not performed in exact values but described qualitatively.

III. Results and discussion

The results were described in two great views. One is the performance dependence of cylindrical thrusters on the channel dimension, and the other is the comparison the performance of the cylindrical thruster to that of the annular thruster.

Fig. 4 shows results of measurements for cylindrical type thrusters classified by their channel dimensions. Discharge currents increased with mass flow rates. For a fixed flow rate, the current distribution spreads out in some range. This represents the amount of the discharge current variation with the discharge voltage change. Altogether, the discharge current of the SI-200Cv2 was higher than that of the SI-200Cv1. That means either the mass utilization of the SI-200Cv2 is better than that of the SI-200Cv1 or the current utilization of the SI-200Cv2 is worse than that of the SI-200Cv1. Thrust and Specific impulse data shows that the former is right. The slopes of thrust distributions of both thrusters are same and also both data are on the same trend line. Also the specific impulse increased with the same trend regardless of the channel dimension. The fact that the thrust per unit mass flow rate of SI-200Cv2 is greater than that of the SI-200Cv1 at fixed flow rate confirms better performance of the SI-200Cv2 in the mass utilization. A visible difference between the SI-200Cv1 and the SI-200Cv2 appears in efficiencies. In the tests, SI-200Cv-series thrusters showed the best performance at different discharge voltages for the different channel dimensions, and it seemed like that the optimal discharge voltage varies with the condition of magnetic field strength. Anyway, efficiencies of the SI-200Cv2 were better than those of the SI-200Cv1 at the low power under 200 W.

Fig. 5 is the summary of several performance tests for all thrusters. The SI-200Cv-series and the SI-200Av1 are different in all aspects of performance details. The difference in slopes in the thrust graph is due to the difference in current changes with voltages. In case of the SI-200Av1 the increase of discharge power means the increase of voltage only, because current does not vary with voltage. On the other hand, for the SI-200Cv-series the voltage increase results in the current increase. Therefore, that the slope of thrust versus power for the SI-200Cv-series is smaller than for the SI-200Av1 shows current increases with voltage increases did not come from the additional

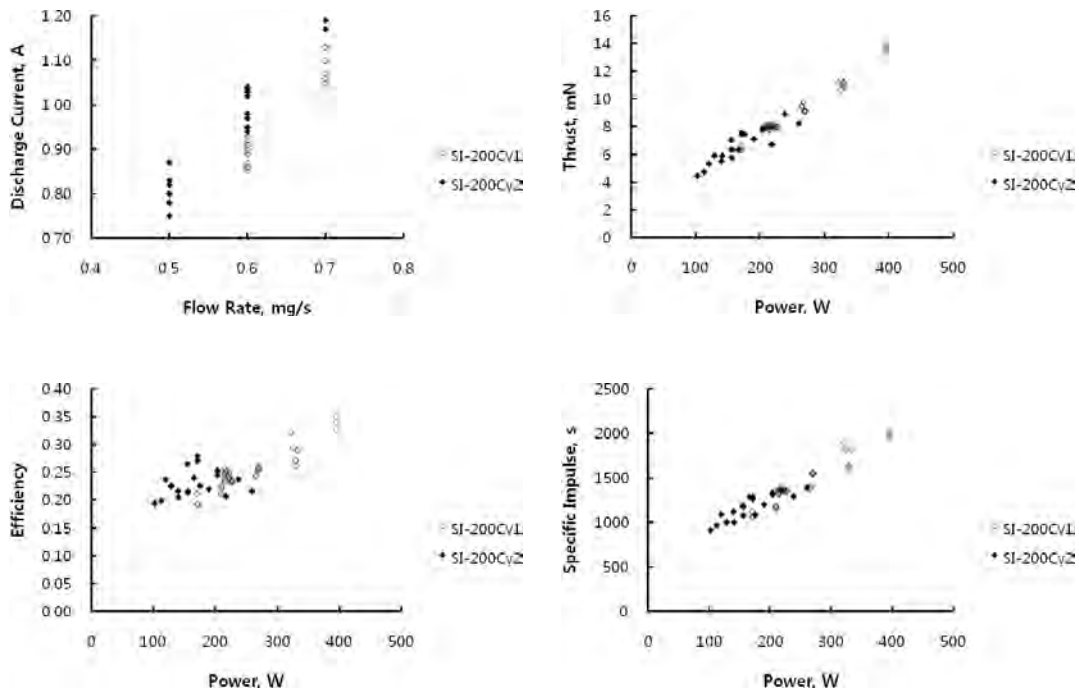


Figure 4. Performance comparison between the SI-200Cv1 in the voltage range of 200-350 V and the SI-200Cv2 in the voltage range of 125-250 V. Full markers denote the SI-200Cv2 and empty markers denote the SI-200Cv1 thruster.

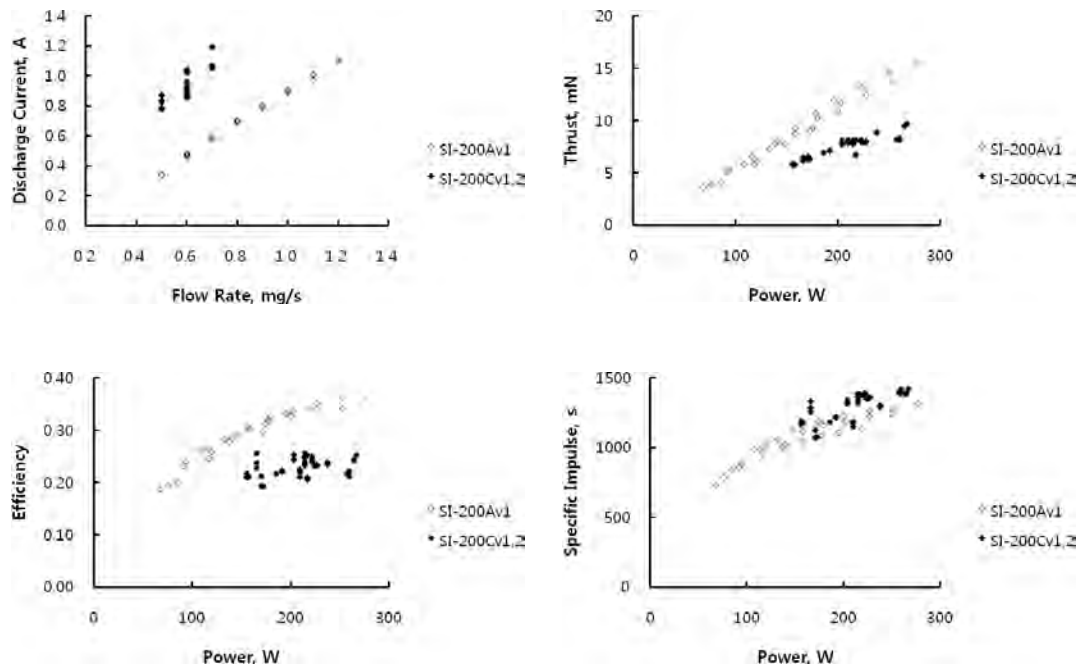


Figure 5. Performance comparison between the SI-200Av1 and the SI-200Cv-series in the voltage range of 200-250 V. Full markers denote the SI-200Cv-series and empty markers denote the SI-200Av1 thruster.

ionization. It is thought that the stagnation of efficiency with the power increasing for the SI-200Cv-series can be explained in the same manner.

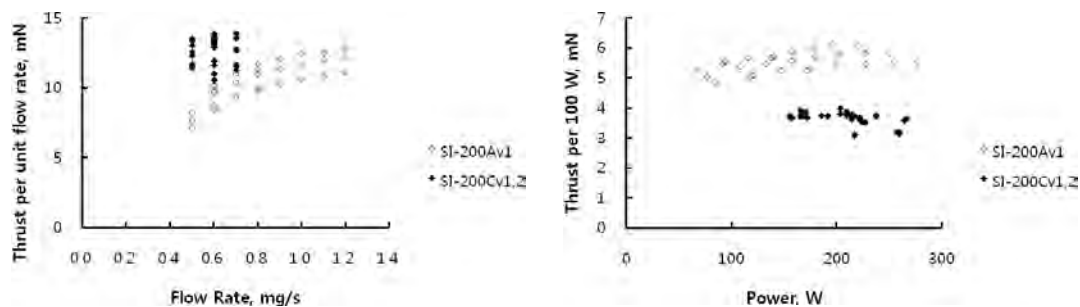


Figure 6. Performance comparison between the SI-200Av1 and the SI-200Cv series in the voltage range of 200-250 V. Full markers denote the SI-200Cv-series and empty markers denote the SI-200Av1 thruster.

A notable difference is that the currents of the SI-200Cv-series are nearly double the SI-200Av1's at the same flow rate. Through the thrust and efficiency results, we concluded that the high current of the SI-200Cv-series came mainly from the bad current utilization which means electron current contribution to discharge current is high. However, it is not all the reason of high current of the SI-200Cv-series. The specific impulses of the SI-200Cv-series are some higher than those of the SI-200Av1 and it means that the thrust force of the SI-200Cv-series are larger than that of the SI-200Av1 at a fixed flow rate. The graph of thrust per unit flow rate versus flow rate in Fig. 6 shows this more clearly. Higher thrust level at the same flow rate means higher mass utilization or higher voltage utilization. Ion current and ion energy data support the fact that the SI-200Cv-series is superior than the SI-200Av1 for both mass utilization and voltage utilization. The right graph in Fig. 6 shows the thrust levels per a discharge power of 100 W. In a view of power consumption, the SI-200Av1 has a comparative advantage. Two graphs in Fig. 6 shows contrastively the clear difference between the SI-200Cv-series and the SI-200Av1.

Fig. 7 shows the ion current density distributions for each SI-200Cv2 and SI-200Av1 at a mass flow rate of 0.6 mg/s and a voltage of 250 V. The ion beam of the SI-200Cv2 diverges more than the SI-200Av1, and the near-axis beam current of the SI-200Cv2 is lower than that of the SI-200Av1. However, the total beam current of the SI-200Cv2 calculated from this ion current distribution was larger than that of the SI-200Av1. That means the SI-200Cv2 is more efficient than the SI-200Av1 in the view of mass utilization or ionization, and this results in the high specific impulse.

Fig. 8 shows the ion energy distributions measured at the thruster axis. In all voltage conditions, peaks of the SI-200Cv2 are positioned at higher energy than the SI-200Av1, and also for the average ion energy, the SI-200Cv2 is higher than the SI-200Av1. This may imply that the voltage utilization of the SI-200Cv2 is higher than that of the SI-200Av1. The width of the energy distribution gives some rough information on the localization of ionization and acceleration zone. Very sharp distribution means that the ionization zone and acceleration zone are well localized. Also, wide width may stand for relatively higher charge density in the ion beam. For all voltages, width for the SI-200Cv2 is wider than for the SI-200Av1. The ionization rate of the SI-200Cv2 calculated from the ion current data is about 90%, but the mass utilization efficiency is estimated about 60%. This tells us that the fraction

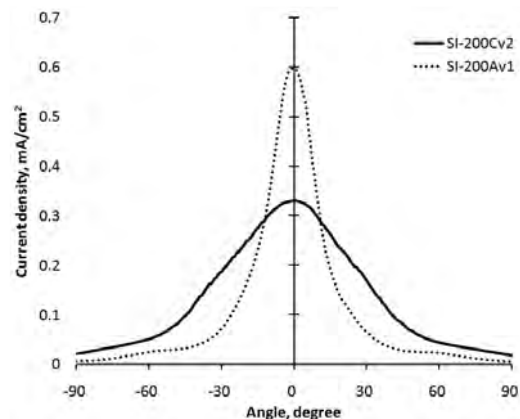


Figure 7. Ion current density distributions for the SI-200Cv2 and the SI-200Av1 at 0.6 mg/s, 250 V.

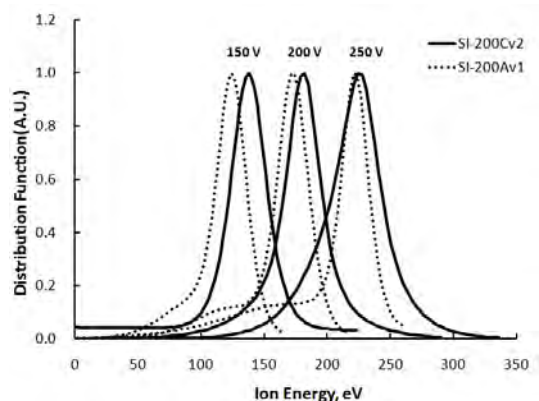


Figure 8. Ion energy distribution for the SI-200Cv2 and the SI-200Av1 on the thruster axis at a mass flow rate of 0.6 mg/s

of multiply charged ions is over the half of entire ions. For the SI-200Av1 the ionization rate is almost same as the mass utilization rate, about 50%. It can be thought that the high fraction of multiply charged ions increases the charge density of the ion beam, and this makes stronger coulomb collisions in the ion beam and so wider width. For instance, at the discharge voltage of 250 V, not only the width of distribution for the SI-200Cv2 is wider than that for the SI-200Av1, but also the portion of ions that have energy over 250 V, that is, the discharge voltage for the SI-200Cv2 is larger than that for the SI-200Av1. We think that these over-energy ions of the SI-200Cv2 came from the higher mass utilization and more multiply charged ions.

IV. Conclusion

In this study, we described the performance characteristics of cylindrical Hall thrusters through the quantitative values of thrust, discharge current, ion current and ion energy, and also through the qualitative utilization efficiency analysis. Though in our experiments two types of thrusters showed the sharp distinction in several performance indicators, additional tests for thrusters in various size and various discharge conditions is needed to generalize the performance characteristics of each thrusters. But, certainly the comparative study on the cylindrical type thruster and the annular type thruster gave us an insight about the development of our low power propulsion device. In low power region our cylindrical type SI-200Cv series have a merit for the mission limited by the propellant mass, but not for the mission limited by the power.

References

- ¹Smirnov, A., Raitses, Y., and Fisch, N. J., "Performance Studies of Miniaturized Cylindrical and Annular Hall Thrusters," *Joint Propulsion Conference*, 2002-3823, AIAA, Indianapolis, IN, 2002.
- ²Polzin, K. A., "Performance of a Low-Power Cylindrical Hall Thruster," *International Electric Propulsion Conference*, 2005-011, IEPC, Princeton, NJ, 2005.
- ³Shirasaki, A., and Tahara, H., "Operational Characteristics and Plasma Measurements in Cylindrical Hall Thrusters," *Journal of Applied Physics*, Vol. 101, No. 073307, 2007.
- ⁴Jacobson, D. T., and Jankovsky, R. S., "Test Results of a 200 W Class Hall Thruster," NASA TM-209447, 1999.
- ⁵Hofer, R. R., Gallimore, A. D., "Efficiency Analysis of a High-Specific Impulse Hall Thruster," *Joint Propulsion Conference*, 2004-3602, AIAA, Lauderdale, FL, 2004.
- ⁶Raitses, Y., Smirnov, A., Fisch, N. J., "Cylindrical Hall Thrusters," *AIAA Plasmadynamics and Lasers Conference*, 2006-3245, AIAA, San Francisco, CA, 2006.
- ⁷Finite Element Method Magnetism, Ver. 8, Aladin Enterprise, Menlo Park, CA, 1999.
- ⁸Mazella, M., Oleson, S., Sankovic, J., Hass, T., Semenkin, and A., Kim, V., "Evaluation of Low Power Hall Thruster Propulsion," NASA TM-107326, 1996.
- ⁹Guerrini, G., Michaut, C., Dudeck, M., Vesselovzorov, A. N., and Bacal, M., "Characterization of Plasma Inside the SPT-50 Channel by Electrostatic Probes," *International Electric Propulsion Conference*, 1997-053, IEPC, Cleveland, OH, 1997.